Efficacy of a Cancer Vaccine against ALK-Rearranged Lung Tumors

Claudia Voena, Matteo Menotti, Cristina Mastini, Filomena Di Giacomo, Dario Livio Longo, Barbara Castella, Maria Elena Boggio Merlo, Chiara Ambrogio, Qi Wang, Valerio Giacomo Minero, Teresa Poggio, Cinzia Martinengo, Lucia D'Amico, Elena Panizza, Luca Mologni, Federica Cavallo, Fiorella Altruda, Mohit Butaney, Marzia Capelletti, Giorgio Inghirami, Pasi A. Jänne, and Roberto Chiarle

Efficacy of a Cancer Vaccine against ALK-Rearranged Lung Tumors

In Cancer Immunol Res. 2015 Dec;3(12):1333-43

DOI: 10.1158/2326-6066.CIR-15-0089

Efficacy of a cancer vaccine against ALK-rearranged lung tumors.

Claudia Voena[1,2], Matteo Menotti[1,2,§], Cristina Mastini[1,2,§], Filomena Di Giacomo[1,2], Dario Livio Longo[1,3], Barbara Castella[1,2], Maria Elena Boggio Merlo[1,2], Chiara Ambrogio[4], Qi Wang[5], Valerio Giacomo Minero[1,2], Teresa Poggio[1,2], Cinzia Martinengo[1,2], Lucia D'Amico[1,2], Elena Panizza[1,2], Luca Mologni[6], Federica Cavallo[1,7], Fiorella Altruda[1,7], Mohit Butaney[8,9], Marzia Capelletti[8,9], Giorgio Inghirami[1,2], Pasi A. Jänne[8,9,10], Roberto Chiarle[1,2,5,*]

[1]Department of Molecular Biotechnology and Health Sciences, University of Torino, Torino, Italy. [2]Center for Experimental Research and Medical Studies (CERMS), Città della Salute e della Scienza, Torino, Italy. [3]Molecular Imaging Center, University of Torino, Torino, Italy. [4]Molecular Oncology Program, Centro Nacional de Investigaciones Oncológicas, Madrid, Spain. [5]Department of Pathology, Children's Hospital Harvard Medical School, Boston, MA 02115, USA. [6]Department of Health Sciences, University of Milano-Bicocca, Milano, Italy; [7]Molecular Biotechnology Center, University of Torino, Torino, Italy. [8]Department of Medical Oncology, Dana-Farber Cancer Institute, Boston, MA 02115, USA. [9]Lowe Center for Thoracic Oncology, Dana-Farber Cancer Institute, Boston, MA 02115, USA. [10]Belfer Institute for Applied Cancer Science, Dana Farber Cancer Institute, Boston, MA 02115, USA

§ equally contributed to this work.

Running title: ALK vaccine in ALK-rearranged NSCLC

Keywords: ALK-DNA vaccine, ALK-rearranged NSCLC, PD-L1, lung cancer immunotherapy

Financial support: The work has been supported by grants FP7 ERC-2009-StG (Proposal No. 242965 - "Lunely") to RC; Associazione Italiana per la Ricerca sul Cancro (AIRC) grant IG-12023 to RC; Koch Institute/DFCC Bridge Project Fund to RC; Ellison Foundation Boston to RC; Worldwide Cancer Research (former AICR) grant 12-0216 to RC and R01 CA136851 to PAJ.

***Corresponding author:**
Roberto Chiarle, M.D.
Department of Pathology, Children's Hospital Boston
Associate Professor in Pathology, Harvard Medical School
Enders 1116.1, 300 Longwood Ave
Boston, MA 02115
Phone: (617) 919-2662
Fax: (617) 730-0148
email: roberto.chiarle@childrens.harvard.edu

The authors declare no competing financial interests.

Abstract

Non-small cell lung cancer (NSCLC) harboring chromosomal rearrangements of the *anaplastic lymphoma kinase* (*ALK*) gene is treated with ALK tyrosine kinase inhibitors (TKIs), but is successful for only a limited amount of time; most cases relapse due to the development of drug resistance. Here we show that a vaccine against ALK induced a strong and specific immune response that both prophylactically and therapeutically impaired the growth of ALK-positive lung tumors in mouse models. The ALK vaccine was efficacious also in combination with ALK TKI treatment and significantly delayed tumor relapses after TKI suspension. We found that lung tumors containing *ALK* rearrangements induced an immunosuppressive microenvironment, regulating the expression of PD-L1 on the surface of lung tumor cells. High PD-L1 expression reduced ALK vaccine efficacy, which could be restored by administration of anti-PD-1 immunotherapy. Thus, combinations of ALK vaccine with TKIs and immune checkpoint blockade therapies might represent a powerful strategy for the treatment of ALK-driven NSCLC.

Introduction

Lung cancer is the leading cause of cancer-related mortality worldwide. In recent years, the identification of key genetic alterations in non-small-cell lung cancer (NSCLC) has prompted the use of rationally targeted therapies, which showed unprecedented clinical benefits (1,2). Approximately 5-6% of NSCLC have chromosomal rearrangements of the *anaplastic lymphoma kinase* (*ALK*) gene that generate different chimeric proteins, such as EML4-ALK, TFG-ALK, and KIF5b-ALK (3-5). In all such fusions, constitutively active ALK acts as a potent tumorigenic driver that activates downstream oncogenic signals, leading to increased cell proliferation and survival (4).

Experimental and clinical data show that *ALK*-rearranged NSCLCs respond to treatment with specific tyrosine kinase inhibitors (TKIs), such as crizotinib (6,7). Despite a high rate of initial response, the development of resistance to crizotinib almost invariably leads to tumor relapse and eventually to the patient's death (8,9). Next-generation ALK TKIs, such as ceritinib and alectinib, have been developed to overcome crizotinib resistance and can further extend survival in crizotinib-resistant patients (10-12). Resistance to ALK TKIs is mediated by point mutations of the ALK kinase domain, by *ALK* gene amplification, or by activation of other compensatory pathways, so-called bypass tracks, such as EGFR, c-KIT, c-MET, and IGF-R1 (8,13-16). Thus, additional therapies to be combined with ALK TKIs are needed to further prolong remission or clinical response in NSCLC patients with *ALK* rearrangements.

Immunotherapy aimed at enhancing the immune response against tumor cells shows promising efficacy in a fraction of NSCLC (17,18). In this context, the ALK protein has many features of an ideal tumor oncoantigen that can be exploited to design specific immunotherapies, such as a cancer vaccine. ALK is required for tumor survival and growth and expressed minimally in some nervous system cells (4,19). ALK is also antigenic in humans, as lymphoma patients with *ALK* rearrangements mount spontaneous B- and T-

cell responses against the ALK protein, with measurable antibodies (20), cytotoxic T lymphocytes (CTLs), and $CD4^+$ T helper effectors to ALK epitopes (21-24). A robust immune response to ALK is associated with a decreased risk of relapse in lymphoma patients (25). Our previous ALK vaccine in pre-clinical mouse models of lymphoma containing *ALK* rearrangements induced specific and potent immune responses that provided strong and durable tumor protection (19).

We here test the efficacy of ALK vaccination in lung cancer. Grafted or primary mouse models of ALK-positive lung tumors demonstrated that an ALK vaccine elicited a strong, ALK-specific CTL response in both mouse models, efficiently blocking tumor growth.

Materials and Methods

Cell Lines and Reagents.

Human *ALK*-rearranged NSCLC cell lines, H2228 (variant 3, E6;A20), DFCI032 and H3122 (variant 1, E13;A20) were obtained from the ATCC collection and were passaged for fewer than 6 months after receipt and resuscitation. These cell lines were further internally tested for the presence of EML-ALK rearrangement. The murine ASB-XIV cell line was purchased from Cell Lines Service (CLS) and was passaged for fewer than 6 months after receipt and resuscitation.

ALK TKIs, NVP-TAE684 was purchased from Axon Medchem and crizotinib (PF-02341066) was kindly gifted by Pfizer.

Mice. Strains of mice used in this study include K-$Ras^{LSL/G12V}$ and Tg $EGFR^{L858R}$, as previously published (26,27), and BALB/c mice (Charles River). Mice were handled and treated in accordance with European Community guidelines.

Generation of ALK Transgenic Mice. A cDNA fragment encoding EML4-ALK (variant 1, E13;A20) or TFG-ALK was ligated to the human SP-C promoter as well as to a polyadenylation signals (Supplementary Figure 1A). The expression cassette was injected into pronuclear-stage embryos of FVB/N mice. The presence of the transgene was examined by PCR analysis with DNA from the tail of founder animals. Mice were handled and treated in accordance with European Community guidelines. Methods are further described in Supplementary Materials and Methods.

DNA Vaccination and *In Vivo* Cytotoxicity Assay. For DNA vaccination, 50 μg of pDEST or pDEST-ALK plasmids were used as previously described (19). The *In Vivo* Cytotoxicity Assay was previously reported(19).

Antibody dosing for *in vivo* treatment

For $CD4^+$ and $CD8^+$ cell depletion, anti-CD4 (clone GK1.5) and anti-CD8 (clone 2.43) antibodies were purchased from BioXcell. For depletion mice were injected i.p. with 100μg of anti-CD4 or anti-CD8 at day -1, +5, +15 and +25.

For PD-1 blockade, anti-PD-1 (clone J43) and control anti-hamster polyclonal IgG for the *in vivo* experiments were purchased from BioXcell. Mice received 200μg of each anti-PD-1 and anti-PD-L1 or 200μg of anti-hamster IgG i.p. every 3 days for a total of 5 injections.

Magnetic Resonance Imaging. MR images were acquired on a Bruker Avance 300 spectrometer operating at 7 T and equipped with a microimaging probe (Bruker Bio-Spin), as described in the Supplementary Materials and Methods.

Histology and Immunohistochemistry. For histological evaluation, tissue samples were fixed in formalin, embedded in paraffin, stained and visualized as previously described(19).

T lymphocytes and T_{reg} cells were quantified by measuring the number of $CD3^+$, $CD8^+$, $CD4^+$ and $Foxp3^+$ cells, respectively, among the total tumor cells.

Intratumoral Cell Characterization. For flow cytometry analysis, lung cell infiltrate was obtained using the Lung Dissociation Kit (Miltenyi Biotec) following manufacturer's instructions. Cells were resuspended in phosphate buffer and stained with antibodies described in Supplementary Materials and Methods.

Statistical Methods. Kaplan-Meier analyses for survival curves were performed with GraphPad Prism 5 and p values were determined with a log-rank Mantel-Cox test. Paired data were compared with the Student's *t* test. P values of <0.05 were considered to be significant. Unless otherwise noted, data are presented as means ± SEM.

Results

ALK vaccination elicits a specific cytotoxic response and prevents tumor growth in an orthotopic model of ALK-positive lung cancer.

To test the efficacy of the ALK vaccine against lung cancer, we developed an orthotopic mouse model of ALK-positive lung cancer by ectopic expression of EML4-ALK in the syngeneic BALB/c murine lung cancer cell line ASB-XIV. We transduced ASB-XIV cells with a retroviral vector containing the EML4-ALK cDNA (variant 1) and green fluorescent protein (GFP) as a reporter. Protein expression in transduced ASB-XIV cells was comparable to EML4-ALK expression in human *ALK*-rearranged NSCLC cells (variant 1 in H3122 and 3 in H2228) (Fig. 1A). ASB-XIV cells express MHC class I and thus are suitable for tumor immune studies (Fig. 1B). Within 3 weeks after i.v. injection of 5×10^5 ASB-XIV cells into the mouse tail vein, tumor nodules were detected in both lungs (Fig. 1,

E and F). We vaccinated BALB/c mice with a DNA plasmid coding for the intracytoplasmic domain of ALK (19) (Fig. 1C).

ALK vaccine induced a strong ALK-specific immune response as measured by an *in vivo* cytotoxic assay (19) (Fig. 1D). Ten days after the second vaccination, we injected EML4-ALK or GFP ASB-XIV cells. GFP ASB-XIV cells gave equal numbers of tumors in mice vaccinated with either a control or the ALK plasmid (Fig. 1E). In contrast, tumors of EML4-ALK ASB-XIV cells had impaired growth in ALK vaccinated mice (Fig. 1F). Thus, ALK vaccination induced an ALK-specific immune response that efficiently prevented the growth of ALK-positive lung tumors.

ALK vaccination delays tumor growth and increases the overall survival of EML4-ALK-rearranged NSCLC Tg mice.

To test the efficacy of the ALK vaccine as a therapy for primary lung tumors, we generated two transgenic (Tg) mouse models of ALK-driven lung cancers. Two rearrangements of *ALK* (EML4-ALK, variant 1, or TFG-ALK) were expressed under the human lung-specific surfactant protein-C (SP-C) promoter (Supplementary Fig. S1A), because human *ALK*-rearranged NSCLC are often SP-C positive (28), and the expression of EML4-ALK by the SP-C promoter can induce efficient lung tumor formation in mice (29). Both transgenic mouse models expressed the ALK fusion selectively in lung epithelial cells, in amounts comparable to human NSCLC with rearranged *ALK* (Supplementary Fig. S1. B-D) and rapidly developed multifocal ALK^+ tumors few weeks after birth, with 100% penetrance (Supplementary Fig. 1, E and F). Tumors were mainly well-differentiated adenocarcinoma growing as papillary, acinar, or more solid carcinoma (30). Ki-67 immunostaining showed that these tumors had a proliferation rate of 10.5% ±1.4 for EML4-ALK and 8.5% ±1.9 for TFG-ALK (Supplementary Fig. S1G). At 4 weeks of age, a few tumor nodules in both ALK mice (Supplementary Fig. S1, H and I, left panels) were detected by magnetic resonance

imaging (MRI). Existing nodules rapidly expanded in volume and new nodules appeared in the lungs over time (Supplementary Fig. S1, H and I, central and right panels). No tumor metastases were detected by examination of other organs with MRI or histology in ALK mice at any age, consistent with other constitutive or ALK-inducible mice (29,31). Both EML4-ALK and TFG-ALK mice died within 50 weeks, with a mean survival of 33.25 weeks for EML4-ALK mice and 37 weeks for TFG-ALK mice (Supplementary Fig. S1L).

To test the efficacy of the ALK vaccine, we screened ALK mice by MRI to stratify them according to their tumor burden. ALK mice were vaccinated at 4 weeks of age, when tumors were detectable in the lungs (Supplementary Fig. S1, H and I), according to the protocol in Fig. 2A. The ALK vaccine generated strong ALK-specific cytotoxic activity in both ALK models, comparable to WT littermates (Fig. 2B). In EML4-ALK mice, the average number of tumors detected in control mice was 58±6.0 by week 20, whereas ALK vaccinated mice had only 16±3.5 at the same time point (Fig. 2, C and D). Similar results were observed in TFG-ALK mice at 20 weeks of age (67±6.0 nodules in control mice compared to 20 ±3.5 nodules in vaccinated mice; Fig. 2E and Supplementary Fig. S2A). Correspondingly, the overall tumor burden calculated in terms of tumor volumes by serial MRI was significantly lower in ALK vaccinated than in control mice (Supplementary Fig. S2, B and C). Survival of ALK vaccinated mice was significantly extended by at least 18 weeks in EML4-ALK and by 12 weeks in TFG-ALK mice (Fig. 2, F and G). The ALK vaccine was still efficacious against larger tumors in older mice (Supplementary Fig. S2D). Thus, ALK-DNA vaccination was a potent controller of growth of primary *ALK*-rearranged lung tumors.

ALK-DNA vaccination increases the number of intratumoral T cells and requires CD8+ T lymphocytes.

Next, we examined how the ALK vaccine shaped the intratumoral immune infiltrate. The ALK vaccine increased the number of intratumoral T cells in both EML4-ALK and TFG-

ALK mice, which was associated with a reduced tumor size (Fig. 3, A and B). Both $CD4^+$ and $CD8^+$ T cells were significantly increased in ALK vaccinated mice (Fig. 3C). In ALK vaccinated mice tumor-infiltrating T cells had a significantly higher $CD8^+/CD4^+$ ratio compared to controls, due to the DNA vaccine preferentially stimulating a $CD8^+$ T cell immune response (Fig. 3C) (32). We also observed an increase in intratumoral T_{reg} cells (Fig. 3, D and E), suggesting that the ALK vaccine induces both T_{eff} and T_{reg} cells, as described for other tumor vaccines (33). Nonetheless, the ratio $CD8^+/Foxp3^+$ was higher in vaccinated mice than in control mice (Fig. 3E).

To confirm that the ALK vaccine required T_{eff} for its anti-tumor functions, we used repeated injections of antibodies specific for $CD4^+$ and $CD8^+$ T cells to deplete them in the orthotopic model based on EML4-ALK ASB-XIV cells (Fig. 3F). The depletion of $CD8^+$ T cells, but not $CD4^+$ T cells, significantly reduced the ALK vaccine efficacy (Fig. 3, G and H). Therefore, in mice bearing ALK-positive tumors, ALK vaccination elicited a cytotoxic response largely mediated by $CD8^+$ T cells. However, in mice depleted of $CD8^+$ T cells the vaccine still appeared to retain some activity, suggesting that other factors may be involved in the immune response elicited by the vaccine.

Immunosuppressive lung microenvironment in ALK-rearranged lung cancer.

We showed that the ALK vaccine stimulates a potent immune response against ALK-rearranged lung tumors. However, the ALK vaccine did not cure the mice, which died after a delay in tumor growth (Fig. 2). Because ALK was still expressed in late tumors, we asked whether the efficacy of the ALK vaccine would diminish over time due to an immunosuppressive microenvironment that progressively develops in lung tumors with *ALK* rearrangements. Indeed, oncogenic activation of EGFR in lung cancers induces an immunosuppressive lung microenvironment by induction of PD-L1 expression on the surface of tumor lung epithelial cells (34).

First, we better characterized the immune infiltrate in mice bearing ALK lung tumors and observed that overall the percentage of B and T lymphocytes, natural killer (NK) cells and granulocytes were comparable between WT and EML4-ALK mice (Supplementary Fig. S3, A-D). However, T cells in tumor bearing EML4-ALK mice displayed a significantly higher expression of PD-1 on both $CD4^+$ and $CD8^+$ T cells (Fig. 4A and Supplementary Fig. S3E) and PD-1^+CD3^+ T cells also expressed other T cell inhibitory molecules such as LAG-3 and TIM-3 in higher amounts (Supplementary Fig. S3E). In addition, $Foxp3^+$ T_{reg} cells were also increased in EML4-ALK mice over time (Supplementary Fig. S3F). These data suggest that tumor lungs bearing EML4-ALK develop an immunosuppressive microenvironment reminiscent of that seen in EGFR-driven lung cancer models (34).

We also characterized the immune microenvironment in human ALK-rearranged NSCLC. NSCLC patients with *ALK* rearrangements had lower percentages of $CD3^+$, $CD4^+$, and $CD8^+$ intratumoral T-cell infiltrate than EGFR-mutated NSCLC (Fig. 4B). These findings were further extended by interrogating gene-expression profiling data from larger series of human NSCLC with different oncogenic mutations. By gene set enrichment analysis, we found lower expression of tumor-infiltrating T-cell related molecules in EML4-ALK NSCLC compared to *EGFR*-mutated, *K-RAS*-mutated or *ALK/RAS/EGFR* non-mutated NSCLC (Fig. 4C). In particular, in *ALK*-rearranged tumors we observed significant depletion of TCR-related molecules such as TCRβ chain, CD3δ, CD3γ, CD3ζ, Lck, of the T cell costimulatory molecules ICOS and CD28, as well as of CD80 and CTLA-4 (Supplementary Fig. S4, A-D).

Blockade of PD-1/PD-L1 pathway restores ALK vaccine efficacy against tumor cells with high levels of PD-L1.

We asked whether oncogenic ALK could also regulate PD-L1 expression on lung tumors. Tumors derived from EML4-ALK mice had higher levels of PD-L1 expression than tumors

originating in mice carrying other NSCLC recurrent mutations, such as the K-Ras^{G12V} (26) and EGFR^{L858R} (27) mice (Supplementary Fig. S5A). Next, we analyzed PD-L1 expression by flow cytometry and showed that tumor epithelial cells (CD45^{-}/EpCAM^{+}) and associated hematopoietic cells (CD45^{+}) in EML4-ALK mice expressed PD-L1 (Supplementary Fig. S5B). To determine whether ALK oncogenic activity directly controlled PD-L1 expression in NSCLC, we treated three *ALK*-rearranged NSCLC cell lines (H3122, H2228 and DFCI032) with crizotinib to inhibit ALK activity (Fig. 5A and Supplementary Fig. S5C). Expression of PD-L1 was detectable in all *ALK*-rearranged cell lines tested and was reduced upon ALK inhibition in all three cell lines (Fig. 5B and Supplementary Fig. S5D). Consistently, also PD-L1 mRNA was down-regulated (Fig. 5C and Supplementary Fig. S5E). To further confirm that PD-L1 expression was driven by ALK activity, and to exclude that PD-L1 down-regulation was mediated by crizotinib inhibition of MET, ROS1, or other off-targets, we knocked down EML4-ALK by a doxycycline inducible shRNA system (16). Again, PD-L1 expression was down-regulated upon EML4-ALK knock-down (Supplementary Fig. S5, F and G). We conclude that in *ALK*-rearranged NSCLC, PD-L1 mRNA and protein was regulated by ALK activity. Another group has recently confirmed these findings (35).

The expression of PD-L1 of the surface of tumor cells impairs anti-tumor activity of the immune system (36). We investigated whether the efficacy of the ALK vaccine could be diminished by the expression of PD-L1 on the surface of the target lung tumor cells. EML4-ALK mice express moderate, but detectable PD-L1, and we observed similar intensity of expression by flow cytometry in EML4-ALK ASB-XIV (Fig. 5D). We reasoned that ALK vaccine efficacy could be hampered when target tumor cells express more PD-L1. We engineered EML4-ALK ASB-XIV cells to express more PD-L1 than parental cells by transduction with a lentivirus containing a murine PD-L1 construct (Fig. 5D). Vaccinated mice were injected with control EML4-ALK ASB-XIV cells or EML4-ALK ASB-XIV cells

expressing high PD-L1. In presence of high PD-L1 expression, the ALK vaccine was less effective in preventing lung tumor growth (Fig. 5E), suggesting that the function of ALK-specific T_{eff} cells was modulated by the amount of PD-L1 on the surface of target lung tumor cells.

To test whether administration of antibody to PD-1 could restore a full efficacy of the ALK vaccine, we treated mice with anti-PD-1 or control IgG (Supplementary Fig. S6A). The treatment with anti-PD-1 alone, as well as control IgG, did not have significant effect on tumor growth and mice developed tumors comparable to controls. In contrast, anti-PD-1 treatment almost completely restored the efficacy of the ALK vaccine (Fig. 5F). These results are consistent with findings that immune checkpoint therapy restores an adaptive immune response best in patients with high PD-L1 expression (37,38).

To show that blockade of the PD-L1/PD-1 immune checkpoint was effective with physiological expression of PD-L1, we tested anti-PD-1 treatment in EML4-ALK mice (Supplementary Figure S6B). We observed a stabilization of tumors immediately at the end of treatment (Fig. 5G) followed by a slower growth rate as compared to control mice (Fig. 5H). These data suggest that immune checkpoint blockade therapy could be efficacious in the physiological tumor microenvironment of *ALK*-rearranged lung tumors.

ALK vaccination is effective in combination with ALK TKIs.

Crizotinib treatment of NSCLC patients with *ALK* rearrangements has had success in clinical trials, supporting the use of ALK TKIs as main therapy for NSCLC (39). A combination of ALK TKIs with the ALK vaccine could be an attractive therapeutic possibility for NSCLC patients. In this context, ALK TKIs could reduce the tumor burden to facilitate the activity of the ALK vaccine. We tested this combination in our ALK mouse models. ALK mice were treated with crizotinib (PF-02341066) for 2 weeks (100mg/kg) and concurrently vaccinated with the ALK or control vaccine (Fig. 6A). The immune response

elicited by the vaccine was not affected by administration of crizotinib, as an equally strong ALK-specific cytotoxic immune response *in vivo* was also detected in ALK-vaccinated mice treated with crizotinib (Fig. 6B). As expected, treatment with crizotinib induced the regression of tumors in both groups within 2 weeks (Fig. 6C, left and central panels, and 6D). At 6 weeks from treatment suspension, tumors relapsed at the same sites in crizotinib treated mice (Fig. 6C, top right panels), while the combination of crizotinib and ALK vaccine delayed tumor recurrence (Fig. 6C, bottom right panels). Indeed, mice treated with crizotinib showed relapses and new tumors at 10 weeks from treatment suspension, whereas in ALK-vaccinated mice relapses and new tumors were less numerous and significantly smaller (Fig. 6, D and E). Similar results were obtained when EML4-ALK mice were vaccinated during treatment with TAE684 (25mg/kg) (Supplementary Fig. S7, A-C). Thus, the ALK vaccine might be efficiently combined with ALK TKI treatment to delay tumor relapse after crizotinib suspension.

ALK vaccination prevents growth of tumors expressing crizotinib-resistant ALK mutations.

Human NSCLC patients treated with ALK TKI almost invariably develop resistance. L1196M, C1156Y, and F1174L are common ALK mutations found in patients relapsing under treatment with crizotinib (8,13,40). Point mutations in the ALK kinase domain have the potential to alter the antigenicity of ALK as they can modify its protein structure. To test the activity of the ALK vaccine against these mutants, we transduced ASB-XIV cells with a retroviral vector containing either the EML4-ALK wild-type (41) or the EML4-ALK mutants (Fig. 7A). Control mice injected with ASB-XIV cells expressing the L1196M, C1156Y or F1174L EML4-ALK mutants rapidly developed tumors in the lungs, whereas ALK vaccination almost completely prevented tumor growth of EML4-ALK WT and all mutants (Figures 7B-E). Therefore, the ALK vaccine is not only efficacious against the EML4-ALK

WT but also against some of the most common EML4-ALK mutants that develop in patients during treatment with crizotinib or ceritinib.

Discussion

In this work we extended our previous findings on the efficacy of a DNA ALK vaccine against ALK-positive lymphoma to *ALK*-rearranged lung cancers. Compared to our previous work, we showed that the ALK vaccine is active not only in tumor grafts but also in primary *ALK*-rearranged NSCLC. Because the SP-C promoter is active since embryonic development (42), these mice are likely tolerant to human ALK. Thus, an important advance from this work is the demonstration that an ALK vaccine can overcome tolerance in mice.

In addition, we showed that the ALK vaccine could be combined with either ALK TKI treatment or the anti-PD-1 antibody. These combinatorial therapies make the ALK vaccine attractive for potential clinical use. Current therapies for *ALK*-rearranged NSCLC, based on crizotinib or next-generation ALK TKIs, achieve a clinical response by arresting tumor progression or inducing tumor regression. However, all patients eventually relapse and die due to development of TKI resistance (11,43).

In this work, we set the stage for the application of an ALK vaccine to further extend progression-free survival in NSCLC patients. The ALK vaccine induced a strong systemic and intratumoral immune response in mouse models of *ALK*-rearranged NSCLC, significantly reducing tumor growth and extending survival of treated mice, regardless of the type of *ALK* translocation (EML4-ALK or TFG-ALK). Simultaneous treatment during vaccination with crizotinib or TAE684 did not affect the ALK immune response achieved by the vaccine. Thus, these data indicate the feasibility of administering an ALK vaccine to NSCLC patients during ALK TKI treatment, possibly when the response is maximal in terms of tumor burden reduction.

Additional advantages of such combination could stem by the potential activity of ALK TKIs in the regulation of the tumor immune microenvironment. We showed that the oncogenic activity of ALK directly regulated PD-L1 expression of the surface of tumor cells. High PD-L1 expression impaired the immune response against ALK elicited by the vaccine (Fig. 5). Therefore, PD-L1 down-regulation by ALK TKI treatment could relieve the inhibitory feed-back on intratumoral T cells and facilitate ALK-specific immune responses. Tumor cell death induced by ALK TKIs could release additional tumor neoantigens, including ALK itself, and thus enhance antitumor immune response (44,45). Further investigation to elucidate the effect of ALK TKIs on the tumor microenvironment is required, but it is intriguing that studies in mouse models and metastatic melanoma patients showed an enhanced anti-tumor immune response after treatment with the selective B-RAF inhibitor (vemurafenib) alone, or in combination with MEK inhibitors (41,46).

The immune microenvironment in ALK-rearranged tumors could be, therefore, a critical factor to the ALK-specific immune responses. We presented data indicating that *ALK*-rearranged mice indeed progressively develop an immunosuppressive tumor microenvironment similar to that induced in mice by oncogenic EGFR (34). Compared to WT mice, *ALK*-rearranged lungs accumulated higher numbers of PD-1^+ T cells that also expressed the exhaustion markers TIM-3 and LAG-3, and showed increased numbers of tumor infiltrating T_{reg} cells. *ALK*-rearranged NSCLC patients also showed a likely immunosuppressive microenvironment in the lungs with reduced tumor infiltrating T cells. In ALK-vaccinated lungs, the tumor infiltrating T_{reg} cells were increased and we detected a population of intratumoral $CD8^+$ T cell with high expression of PD-1 (Supplementary Fig. S8, A and B), that we interpreted as exhausted $CD8^+$ T cells, that had been elicited by the ALK vaccine to recognize the ALK antigen (47). In mice with advanced tumors, the ALK vaccine elicited a weaker ALK-specific cytotoxic response (Supplementary Fig. S8C) and decreased anti-tumor activity (Supplementary Fig.S2D). In these settings, T_{reg} depletion by

an antibody to CD25 could partially restore the impaired cytotoxic activity generated by the ALK vaccine (Supplementary Fig. S8C), indicating that T_{reg} cells could also play a critical role in the immunosuppressive tumor environment seen in *ALK*-rearranged lung tumors. Similarly, the restoration of the ALK vaccine efficacy by administration of antibody to PD-1 in high-PD-L1 EML4-ALK ASB-XIV xenografts (Fig. 5) suggests that blockade of immune checkpoint molecules could powerfully potentiate the ALK vaccine.

Overall, these data suggest that combination therapy of ALK TKIs and ALK vaccine could work efficiently in the clinical setting to generate a strong and long-lasting immune response to ALK in NSCLC. The benefit from combined ALK TKI and ALK vaccine therapy can be enhanced by additional immunotherapies, such as anti-PD-1/PD-L1 and anti-CTLA to block immune checkpoints (17,18) or through T_{reg} depletion by antibodies to CD25 (48). Thus, the development of an ALK vaccine for clinical use together with additional immunotherapeutic tools provides exciting therapeutic options for the treatment of *ALK*-rearranged NSCLC.

Acknowledgments

We would like to thank Glenn Dranoff for helpful discussions, Maria Stella Scalzo for technical support, Flavio Cristofani for mice housing and care, Carlo Gambacorti-Passerini for kindly providing critical reagents, Silvio Aime for the Molecular Imaging Facility and Sharmila Fagoonee and Maddalena Iannicella for technical help in transgenic mice generation.

References

1. Pao W, Girard N. New driver mutations in non-small-cell lung cancer. Lancet Oncol 2011;12(2):175-80.
2. Berge EM, Doebele RC. Targeted therapies in non-small cell lung cancer: emerging oncogene targets following the success of epidermal growth factor receptor. Seminars in oncology 2014;41(1):110-25.
3. Soda M, Choi YL, Enomoto M, Takada S, Yamashita Y, Ishikawa S, et al. Identification of the transforming EML4-ALK fusion gene in non-small-cell lung cancer. Nature 2007;448(7153):561-6.
4. Chiarle R, Voena C, Ambrogio C, Piva R, Inghirami G. The anaplastic lymphoma kinase in the pathogenesis of cancer. Nature reviews Cancer 2008;8(1):11-23.
5. Mano H. ALKoma: a cancer subtype with a shared target. Cancer discovery 2012;2(6):495-502.
6. McDermott U, Iafrate AJ, Gray NS, Shioda T, Classon M, Maheswaran S, et al. Genomic alterations of anaplastic lymphoma kinase may sensitize tumors to anaplastic lymphoma kinase inhibitors. Cancer research 2008;68(9):3389-95.
7. Kwak EL, Bang YJ, Camidge DR, Shaw AT, Solomon B, Maki RG, et al. Anaplastic lymphoma kinase inhibition in non-small-cell lung cancer. The New England journal of medicine 2010;363(18):1693-703.
8. Choi YL, Soda M, Yamashita Y, Ueno T, Takashima J, Nakajima T, et al. EML4-ALK mutations in lung cancer that confer resistance to ALK inhibitors. The New England journal of medicine 2010;363(18):1734-9.
9. Shaw AT, Kim DW, Nakagawa K, Seto T, Crino L, Ahn MJ, et al. Crizotinib versus chemotherapy in advanced ALK-positive lung cancer. The New England journal of medicine 2013;368(25):2385-94.
10. Solomon B, Wilner KD, Shaw AT. Current status of targeted therapy for anaplastic lymphoma kinase-rearranged non-small cell lung cancer. Clinical pharmacology and therapeutics 2014;95(1):15-23.
11. Shaw AT, Kim DW, Mehra R, Tan DS, Felip E, Chow LQ, et al. Ceritinib in ALK-rearranged non-small-cell lung cancer. The New England journal of medicine 2014;370(13):1189-97.
12. Friboulet L, Li N, Katayama R, Lee CC, Gainor JF, Crystal AS, et al. The ALK inhibitor ceritinib overcomes crizotinib resistance in non-small cell lung cancer. Cancer discovery 2014;4(6):662-73.

13. Katayama R, Shaw AT, Khan TM, Mino-Kenudson M, Solomon BJ, Halmos B, et al. Mechanisms of acquired crizotinib resistance in ALK-rearranged lung Cancers. Science translational medicine 2012;4(120):120ra17.
14. Lovly CM, McDonald NT, Chen H, Ortiz-Cuaran S, Heukamp LC, Yan Y, et al. Rationale for co-targeting IGF-1R and ALK in ALK fusion-positive lung cancer. Nature medicine 2014;20(9):1027-34.
15. Doebele RC, Pilling AB, Aisner DL, Kutateladze TG, Le AT, Weickhardt AJ, et al. Mechanisms of resistance to crizotinib in patients with ALK gene rearranged non-small cell lung cancer. Clinical cancer research 2012;18(5):1472-82.
16. Voena C, Di Giacomo F, Panizza E, D'Amico L, Boccalatte FE, Pellegrino E, et al. The EGFR family members sustain the neoplastic phenotype of ALK+ lung adenocarcinoma via EGR1. Oncogenesis 2013;2:e43.
17. Topalian SL, Hodi FS, Brahmer JR, Gettinger SN, Smith DC, McDermott DF, et al. Safety, activity, and immune correlates of anti-PD-1 antibody in cancer. The New England journal of medicine 2012;366(26):2443-54.
18. Brahmer JR, Tykodi SS, Chow LQ, Hwu WJ, Topalian SL, Hwu P, et al. Safety and activity of anti-PD-L1 antibody in patients with advanced cancer. The New England journal of medicine 2012;366(26):2455-65.
19. Chiarle R, Martinengo C, Mastini C, Ambrogio C, D'Escamard V, Forni G, et al. The anaplastic lymphoma kinase is an effective oncoantigen for lymphoma vaccination. Nature medicine 2008;14(6):676-80.
20. Pulford K, Falini B, Banham AH, Codrington D, Roberton H, Hatton C, et al. Immune response to the ALK oncogenic tyrosine kinase in patients with anaplastic large-cell lymphoma. Blood 2000;96(4):1605-7.
21. Passoni L, Scardino A, Bertazzoli C, Gallo B, Coluccia AM, Lemonnier FA, et al. ALK as a novel lymphoma-associated tumor antigen: identification of 2 HLA-A2.1-restricted CD8+ T-cell epitopes. Blood 2002;99(6):2100-6.
22. Ait-Tahar K, Cerundolo V, Banham AH, Hatton C, Blanchard T, Kusec R, et al. B and CTL responses to the ALK protein in patients with ALK-positive ALCL. International journal of cancer 2006;118(3):688-95.
23. Ait-Tahar K, Barnardo MC, Pulford K. CD4 T-helper responses to the anaplastic lymphoma kinase (ALK) protein in patients with ALK-positive anaplastic large-cell lymphoma. Cancer research 2007;67(5):1898-901.

24. Passoni L, Gallo B, Biganzoli E, Stefanoni R, Massimino M, Di Nicola M, et al. In vivo T-cell immune response against anaplastic lymphoma kinase in patients with anaplastic large cell lymphomas. Haematologica 2006;91(1):48-55.
25. Ait-Tahar K, Damm-Welk C, Burkhardt B, Zimmermann M, Klapper W, Reiter A, et al. Correlation of the autoantibody response to the ALK oncoantigen in pediatric anaplastic lymphoma kinase-positive anaplastic large cell lymphoma with tumor dissemination and relapse risk. Blood 2010;115(16):3314-9.
26. Guerra C, Mijimolle N, Dhawahir A, Dubus P, Barradas M, Serrano M, et al. Tumor induction by an endogenous K-ras oncogene is highly dependent on cellular context. Cancer cell 2003;4(2):111-20.
27. Politi K, Zakowski MF, Fan PD, Schonfeld EA, Pao W, Varmus HE. Lung adenocarcinomas induced in mice by mutant EGF receptors found in human lung cancers respond to a tyrosine kinase inhibitor or to down-regulation of the receptors. Genes & development 2006;20(11):1496-510.
28. Kim H, Jang SJ, Chung DH, Yoo SB, Sun P, Jin Y, et al. A comprehensive comparative analysis of the histomorphological features of ALK-rearranged lung adenocarcinoma based on driver oncogene mutations: frequent expression of epithelial-mesenchymal transition markers than other genotype. PloS one 2013;8(10):e76999.
29. Soda M, Takada S, Takeuchi K, Choi YL, Enomoto M, Ueno T, et al. A mouse model for EML4-ALK-positive lung cancer. Proceedings of the National Academy of Sciences of the United States of America 2008;105(50):19893-7.
30. Ambrogio C, Carmona FJ, Vidal A, Falcone M, Nieto P, Romero OA, et al. Modeling lung cancer evolution and preclinical response by orthotopic mouse allografts. Cancer research 2014;74(21):5978-88.
31. Chen Z, Sasaki T, Tan X, Carretero J, Shimamura T, Li D, et al. Inhibition of ALK, PI3K/MEK, and HSP90 in murine lung adenocarcinoma induced by EML4-ALK fusion oncogene. Cancer research 2010;70(23):9827-36.
32. Quakkelaar ED, Melief CJ. Experience with synthetic vaccines for cancer and persistent virus infections in nonhuman primates and patients. Advances in immunology 2012;114:77-106.
33. Jacob JB, Quaglino E, Radkevich-Brown O, Jones RF, Piechocki MP, Reyes JD, et al. Combining human and rat sequences in her-2 DNA vaccines blunts immune tolerance and drives antitumor immunity. Cancer research 2010;70(1):119-28.

34. Akbay EA, Koyama S, Carretero J, Altabef A, Tchaicha JH, Christensen CL, et al. Activation of the PD-1 pathway contributes to immune escape in EGFR-driven lung tumors. Cancer discovery 2013;3(12): 1355-63.
35. Ota K, Azuma K, Kawahara A, Hattori S, Iwama E, Tanizaki J, et al. Induction of PD-L1 Expression by the EML4-ALK Oncoprotein and Downstream Signaling Pathways in Non-Small Cell Lung Cancer. Clinical cancer research 2015.
36. Peggs KS, Quezada SA, Allison JP. Cell intrinsic mechanisms of T-cell inhibition and application to cancer therapy. Immunological reviews 2008;224:141-65.
37. Herbst RS, Soria JC, Kowanetz M, Fine GD, Hamid O, Gordon MS, et al. Predictive correlates of response to the anti-PD-L1 antibody MPDL3280A in cancer patients. Nature 2014;515(7528):563-7.
38. Garon EB, Rizvi NA, Hui R, Leighl N, Balmanoukian AS, Eder JP, et al. Pembrolizumab for the treatment of non-small-cell lung cancer. The New England journal of medicine 2015;372(21):2018-28.
39. Shaw AT, Engelman JA. ALK in lung cancer: past, present, and future. Journal of clinical oncology 2013;31(8):1105-11.
40. Friboulet L, Li N, Katayama R, Lee CC, Gainor JF, Crystal AS, et al. The ALK inhibitor ceritinib overcomes crizotinib resistance in non-small cell lung cancer. Cancer discovery 2014;4(6):662-73.
41. Frederick DT, Piris A, Cogdill AP, Cooper ZA, Lezcano C, Ferrone CR, et al. BRAF Inhibition Is Associated with Enhanced Melanoma Antigen Expression and a More Favorable Tumor Microenvironment in Patients with Metastatic Melanoma. Clin Cancer Res 2013;19(5):1225-31.
42. Simonet WS, DeRose ML, Bucay N, Nguyen HQ, Wert SE, Zhou L, et al. Pulmonary malformation in transgenic mice expressing human keratinocyte growth factor in the lung. Proceedings of the National Academy of Sciences of the United States of America 1995;92(26):12461-5.
43. Shaw AT, Engelman JA. Ceritinib in ALK-rearranged non-small-cell lung cancer. The New England journal of medicine 2014;370(26):2537-9.
44. Vanneman M, Dranoff G. Combining immunotherapy and targeted therapies in cancer treatment. Nature reviews Cancer 2012;12(4):237-51.
45. Kroemer G, Galluzzi L, Kepp O, Zitvogel L. Immunogenic cell death in cancer therapy. Annu Rev Immunol 2013;31:51-72.

46. Knight DA, Ngiow SF, Li M, Parmenter T, Mok S, Cass A, et al. Host immunity contributes to the anti-melanoma activity of BRAF inhibitors. J Clin Invest 2013;123(3):1371-81.
47. Yadav M, Jhunjhunwala S, Phung QT, Lupardus P, Tanguay J, Bumbaca S, et al. Predicting immunogenic tumour mutations by combining mass spectrometry and exome sequencing. Nature 2014;515(7528):572-6.
48. Rech AJ, Mick R, Martin S, Recio A, Aqui NA, Powell DJ, Jr., et al. CD25 blockade depletes and selectively reprograms regulatory T cells in concert with immunotherapy in cancer patients. Science translational medicine 2012;4(134):134ra62.

Figure Legends

Figure 1. Prophylactic ALK vaccine prevents the growth of ALK-positive lung tumors in an orthotopic model. A, EML4-ALK expression in ASB-XIV infected cells and in human EML4-ALK NSCLC cell lines (H3122 and H2228) was evaluated by immunoblotting with the indicated antibodies. B, Analysis of the Major Histocompatibility Complex (MHC) Class I (PE-H2D^{d} Ab) antigen expression on ASB-XIV cells by flow cytometry. C, Schematic representation of ALK vaccination protocol in BALB/c mice. Control mice were vaccinated with empty pDEST (Ctrl) and ALK vaccinated mice were vaccinated with pDEST-ALK (Vax). D, Cytotoxic activity in ALK vaccinated mice evaluated by an *in vivo* cytotoxicity assay. Horizontal bars represent means. E and F, Representative hematoxilin-eosin (H&E) sections of lungs injected with GFP-ASB-XIV cells (E) or EML4-ALK ASB-XIV cells (F). Histograms represent the number of tumors in control (Ctrl; n=3 mice) and ALK vaccinated mice (Vax; n=3 mice). Scale bars, 1mm (top) and 50μm (bottom). The total number of tumors was counted in the whole lung of each mouse. Data are represented from three independent experiments as mean (±SEM). ***, P<0.0001.

Figure 2. Therapeutic ALK vaccine delays tumor progression in *ALK*-rearranged NSCLC.

A, ALK vaccination protocol in ALK Tg mice. MRI, Magnetic Resonance Imaging. B, Cytotoxic activity in control mice (○) and ALK vaccinated (Vax) WT mice (□) or Tg mice (■). Horizontal bars represent means. C, Representative coronal MRI sections of lungs from EML4-ALK mice. D and E, Number of tumors in control (Ctrl) and ALK vaccinated (Vax) mice as measured by MRI at the indicated time points. EML4-ALK mice (D, Ctrl = 24 mice; Vax = 26 mice) from three independent experiments. TFG-ALK mice (E, Ctrl = 5 mice; Vax = 9 mice) from two independent experiments. The average number of tumors

for each cohort (± SEM) is displayed. F and G, Overall survival by Kaplan-Meier curves in EML4-ALK mice (F) and TFG-ALK mice (G). **, *P*<0.005; ***, *P*<0.0005; ****, *P*<0.0001.

Figure 3. ALK vaccine increases the number of intratumoral T lymphocytes and depends on cytotoxic CD8$^+$ T cells. A, Representative hematoxilin-eosin (H&E) and immunostaining with anti-CD3 antibody of lung sections from control (Ctrl) and ALK vaccinated (Vax) EML4-ALK mice. Scale bars, 100μm. B, Histograms represent the percentage of CD3$^+$ cells infiltrating the tumors in control (Ctrl) and ALK vaccinated mice (Vax) in EML4-ALK (left) and in TFG-ALK (right) mice at 12 weeks of age. C, Histograms represent the mean percentages of CD8$^+$ and CD4$^+$ T cells infiltrating the tumors and the CD8$^+$/CD4$^+$ ratio in control and vaccinated EML4-ALK mice at 12 weeks of age. D, Representative immunostaining with anti-Foxp3 antibody of lung sections from EML4-ALK control (Ctrl) and ALK vaccinated (Vax) mice (left). Scale bars, 100μm. E, Mean percentages of intratumoral T_{reg} cells (Foxp3$^+$ cells; left) and CD8$^+$/Foxp3$^+$ cell ratio (right) in control and vaccinated EML4-ALK mice. F, Schematic representation of the vaccination protocol in combination with CD4$^+$ or CD8$^+$cell depletion. G, Mean lung tumor numbers (n= 5 mice for each group). Data are from two independent experiments. H, Representative lung sections of ALK vaccinated mice in combination with CD4$^+$ cell depletion or CD8$^+$cell depletion. Data are represented as mean (±SEM). *, *P*<0.05; ****, *P*<0.0001.

Figure 4. ALK induces an immunosuppressive microenvironment in ALK-rearranged NSCLC. A, Lung immune infiltrates were stained with antibodies to CD3, CD4, CD8, PD-1 and analyzed by flow cytometry. Histograms show the mean percentage for each indicated population in WT mice (□, n= 5 mice), 12-week-old EML4-ALK mice (□, n= 5 mice) and 16-week-old EML4-ALK mice (■, n=9 mice). B, Immunohistochemistry for CD3, CD4 and CD8 on a representative mutated EGFR (ex19del) patient (left panels) and a

representative EML4-ALK positive NSCLC case (right panels). Scale bars, 100μm. Graphs show the percentages of CD3+, CD4+ and CD8+ cells in EML4-ALK positive NSCLC *vs* EGFR mutated patients. Horizontal bars represent means. C, Gene Set Enrichment Analysis (GSEA) for T cell markers based on gene expression profiling of human EML4-ALK NSCLC *vs* EGFR mutated NSCLC (L858R or EGFR-Del19) (FDR q-Value: 0.008, top panel) or *vs* K-RAS mutated NSCLC (FDR q-Value: 0.001, central panel) or *vs* K-RAS/EGFR/ALK negative NSCLC (FDR q-Value: 0.00046, bottom panel). *, $P<0.05$; **, $P<0.005$; ***, $P<0.0005$.

Figure 5. Blockade of the PD-1/PD-L1 pathway restores the efficacy of the ALK vaccine against cells expressing high PD-L1. A, Western blot of H3122 cells treated with different crizotinib concentrations and collected at the indicated time points. Membranes were blotted with the indicated antibodies. B, PD-L1 protein expression was evaluated by flow cytometry in H3122 cells treated with 150nM crizotinib for 24 hours. C, PD-L1 mRNA expression was evaluated by qRT-PCR in crizotinib-treated cells. D, PD-L1 expression was evaluated by flow cytometry in ASB-XIV cells (Ctrl), EML4-ALK ASB-XIV (EML-ALK) and in EML4-ALK ASB-XIV transduced with PD-L1 (EML4-ALK/PD-L1). E, Mean tumor numbers in lungs from mice injected with the indicated ASB-XIV cells (n= 5 mice for each group). F, Mean tumor numbers in lungs from mice with the indicated treatments (n= 6-8 mice for each group). Data are represented as mean (±SEM). G and H, Quantification of volume changes compared to baseline tumors in ALK mice treated with control IgG (n=6 mice) or anti-PD-1 antibody (n=7 mice) at the end of treatment (G) and at 4 weeks after treatment suspension (H). Horizontal bars represent means. Data are from two independent experiments. *, $P<0.05$; **, $P<0.005$; ***, $P<0.0005$.

Figure 6. ALK vaccine is efficacious in combination with crizotinib treatment. A, Schematic representation of the ALK vaccination combined with crizotinib treatment in EML4-ALK mice. B, Cytotoxic activity in ALK vaccinated mice in combination with crizotinib. Horizontal bars represent means. C, Representative MRI of crizotinib-treated mice and crizotinib-treated plus vaccinated mice. Arrows indicate tumor recurrence in the same position. Arrowheads indicate new tumors. D and E, The number of tumors (D) and the tumor volume (E) were measured by MRI analysis at the indicated time points. Data are from two independent experiments. Data are represented as mean (±SEM). **, $P<0.005$; ***, $P<0.0005$.

Figure 7. ALK vaccine is effective in tumors with crizotinib resistant EML4-ALK mutants. A, Western Blot shows the expression of EML4-ALK wild-type or the EML4-ALK mutants (C1156Y, F1174L and L1196M) in ASB-XIV infected cells and in human ALK-rearranged NSCLC cell line (H3122). The lines between the blots indicate cut lanes on the same gel. B-E, Representative H&E sections of the lungs of control (Ctrl) and ALK vaccinated (Vax) mice at day 21 after injection i.v. of ASB-XIV cells infected with a GFP plasmid expressing EML4-ALK WT (B) or the EML4-ALK mutants C1156Y (C), L1196M (D) or F1174L (E). Histograms represent the number of tumors in control (Ctrl; n=3 mice for each EML4-ALK construct) and ALK vaccinated mice (Vax; n=3 mice for each EML4-ALK construct). Scale bars, 1mm. Data are from two independent experiments. Data are represented as mean (±SEM). *, $P<0.05$; **, $P<0.005$; ***, $P<0.0005$.

Figure 1

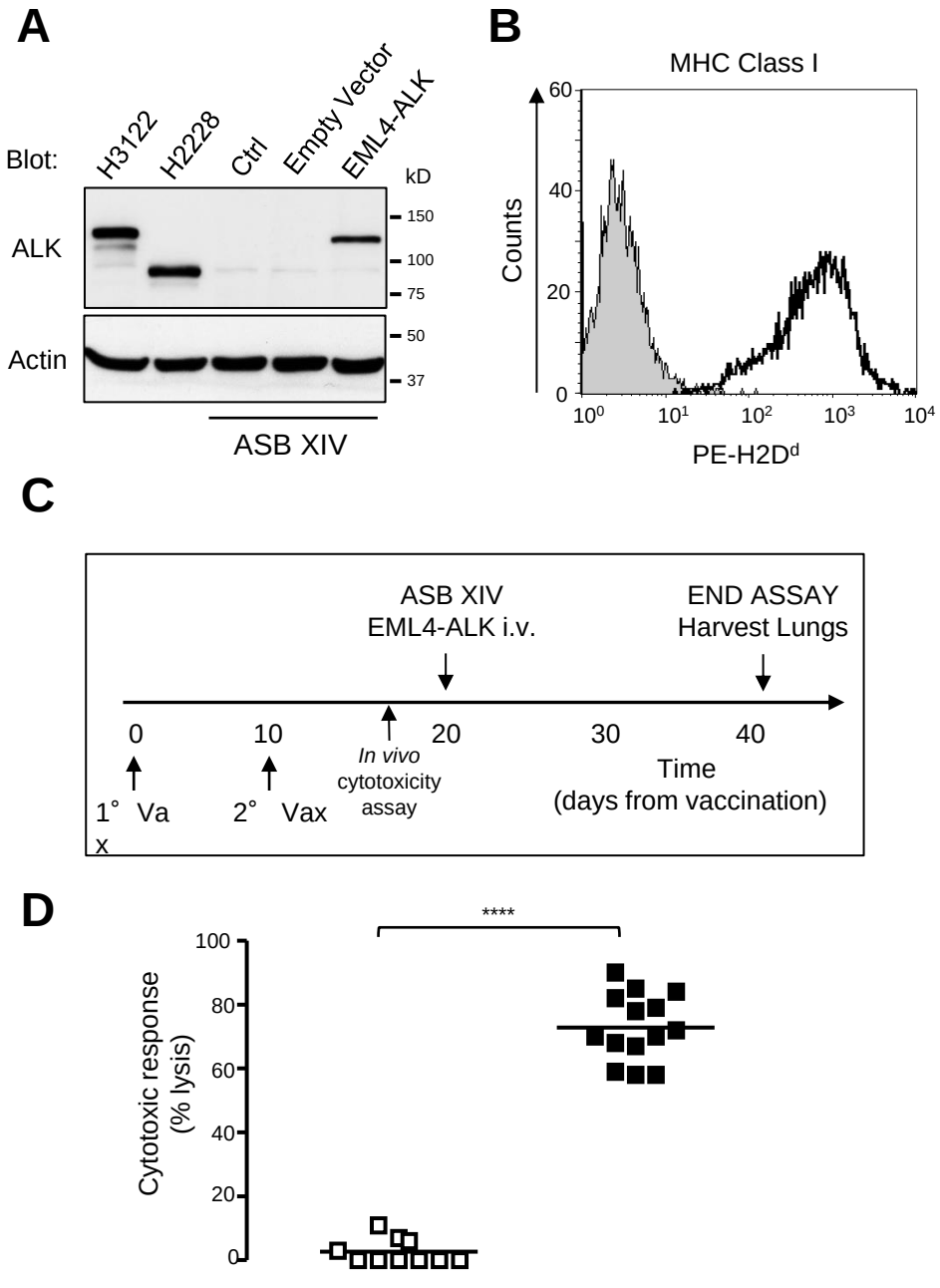
A
Blot:
H3122
H2228
Ctrl
Empty Vector
EML4-ALK
kD
ALK
Actin
150
100
75
50
37
ASB XIV
B
MHC Class I
Counts
60
40
20
0
10^0
10^1
10^2
10^3
10^4
PE-H2D^d
C
ASB XIV
EML4-ALK i.v.
END ASSAY
Harvest Lungs
0
10
20
30
40
1° Va x
2° Vax
In vivo cytotoxicity assay
Time (days from vaccination)
D
Cytotoxic response (% lysis)
****
100
80
60
40
20
0
Ctrl
Vax
E
EMPTY VECTOR
Ctrl
Vax
n. s.
N° of tumors
300
200
100
0
Ctrl
Vax
F
EML4-ALK
Ctrl
Vax
N° of tumors
****
250
200
150
100
50
0
Ctrl
Vax

Figure 2

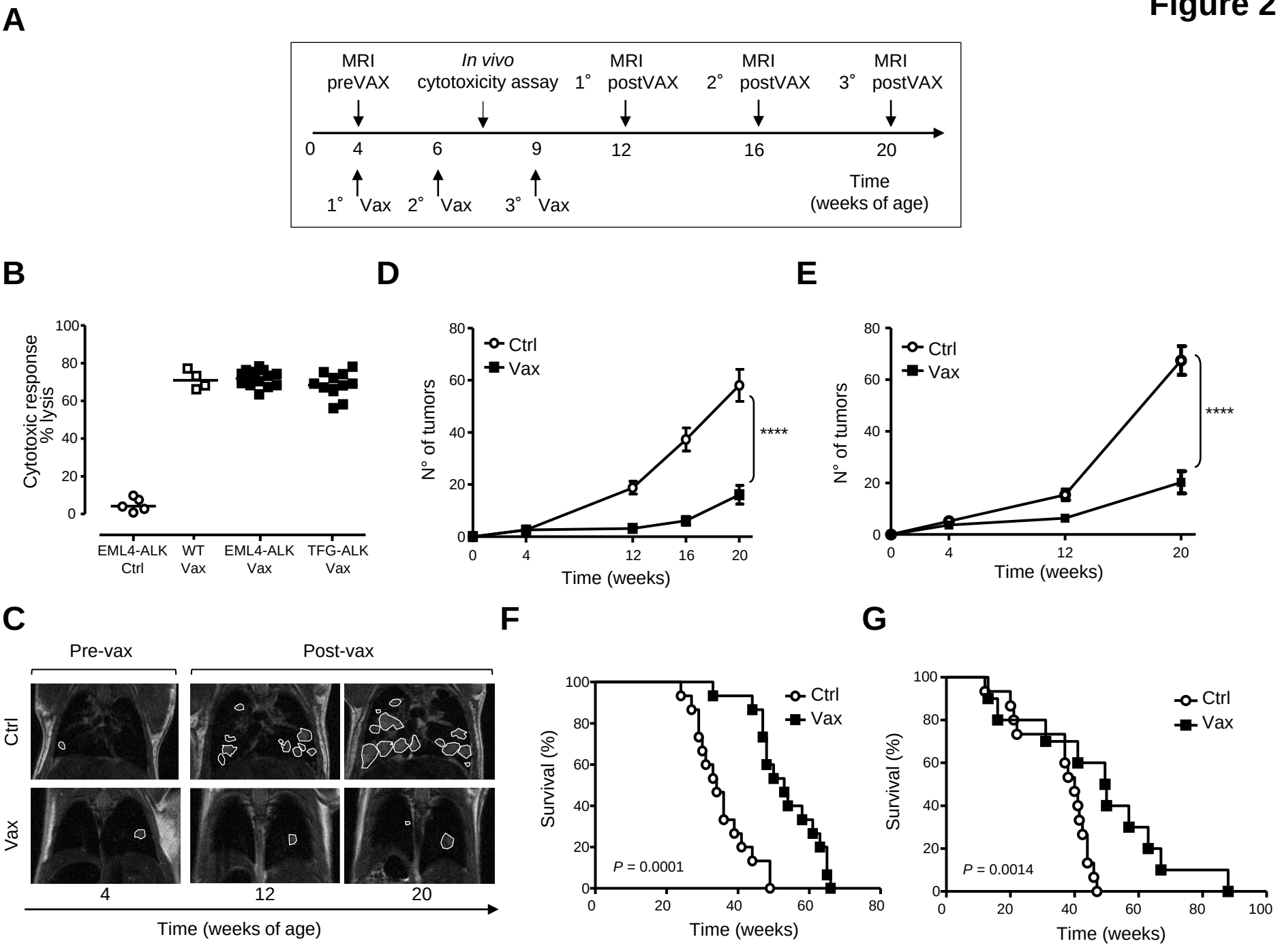
A
MRI preVAX
In vivo cytotoxicity assay
1° MRI postVAX
2° MRI postVAX
3° MRI postVAX
0 4 6 9 12 16 20
Time (weeks of age)
1° Vax
2° Vax
3° Vax
B
Cytotoxic response % lysis
EML4-ALK Ctrl
WT Vax
EML4-ALK Vax
TFG-ALK Vax
D
N° of tumors
Ctrl
Vax
****
Time (weeks)
E
N° of tumors
Ctrl
Vax
****
Time (weeks)
C
Pre-vax
Post-vax
Ctrl
Vax
4
12
20
Time (weeks of age)
F
Survival (%)
Ctrl
Vax
P = 0.0001
Time (weeks)
G
Survival (%)
Ctrl
Vax
P = 0.0014
Time (weeks)

Figure 3

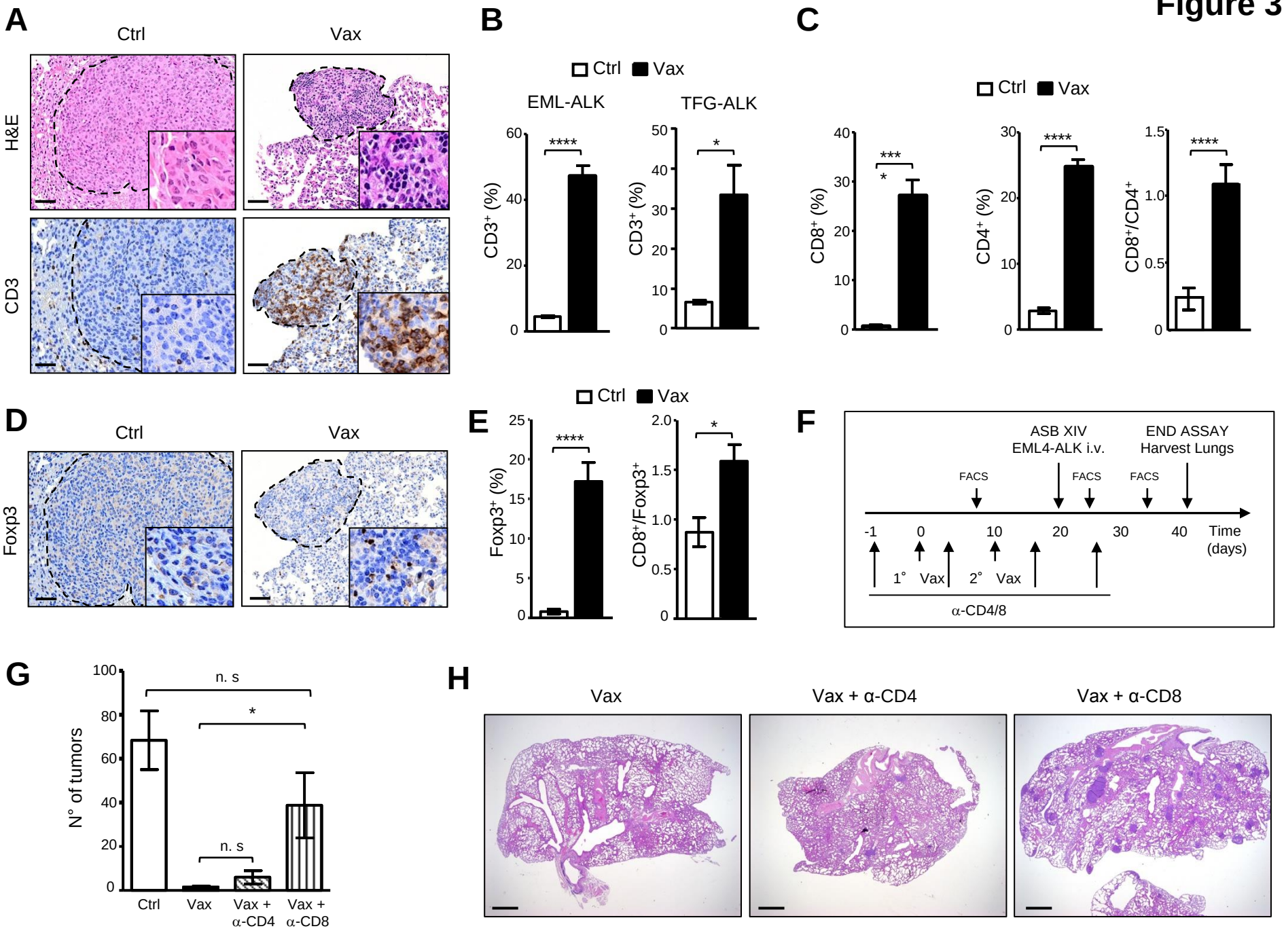
A
Ctrl
Vax
H&E
CD3
B
Ctrl
Vax
EML-ALK
TFG-ALK
CD3+ (%)
****
*
C
Ctrl
Vax
CD8+ (%)
CD4+ (%)
CD8+/CD4+
***
*
****
D
Ctrl
Vax
Foxp3
E
Ctrl
Vax
Foxp3+ (%)
CD8+/Foxp3+
****
*
F
ASB XIV
EML4-ALK i.v.
END ASSAY
Harvest Lungs
FACS
FACS
FACS
-1
0
10
20
30
40
Time
(days)
1° Vax
2° Vax
α-CD4/8
G
N° of tumors
n. s
*
n. s
Ctrl
Vax
Vax +
α-CD4
Vax +
α-CD8
H
Vax
Vax + α-CD4
Vax + α-CD8

Figure 4

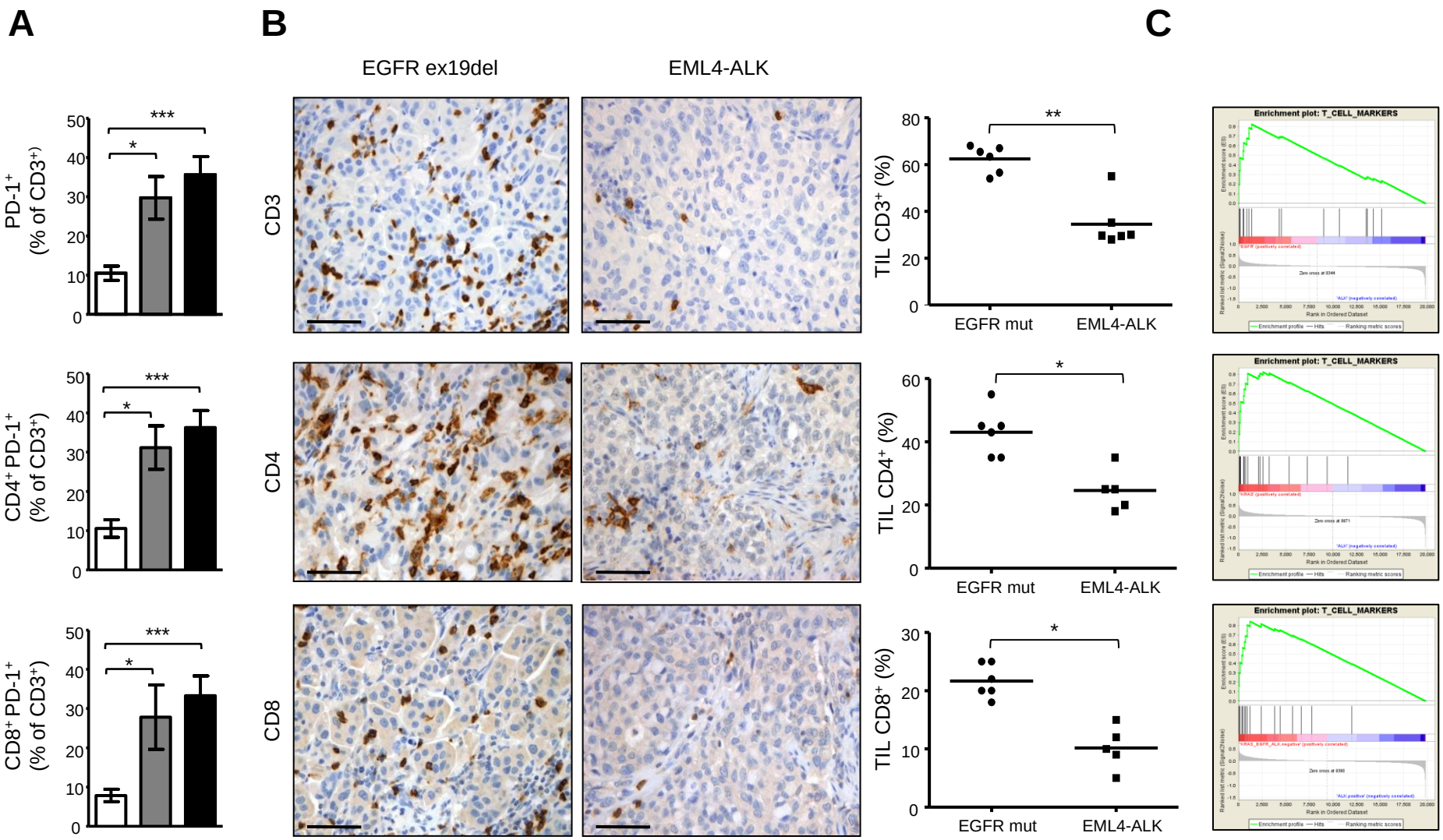
A
B
C
EGFR ex19del
EML4-ALK
PD-1+ (% of CD3+)
CD4+ PD-1+ (% of CD3+)
CD8+ PD-1+ (% of CD3+)
CD3
CD4
CD8
TIL CD3+ (%)
TIL CD4+ (%)
TIL CD8+ (%)
EGFR mut
EML4-ALK
Enrichment plot: T_CELL_MARKERS

Figure 5

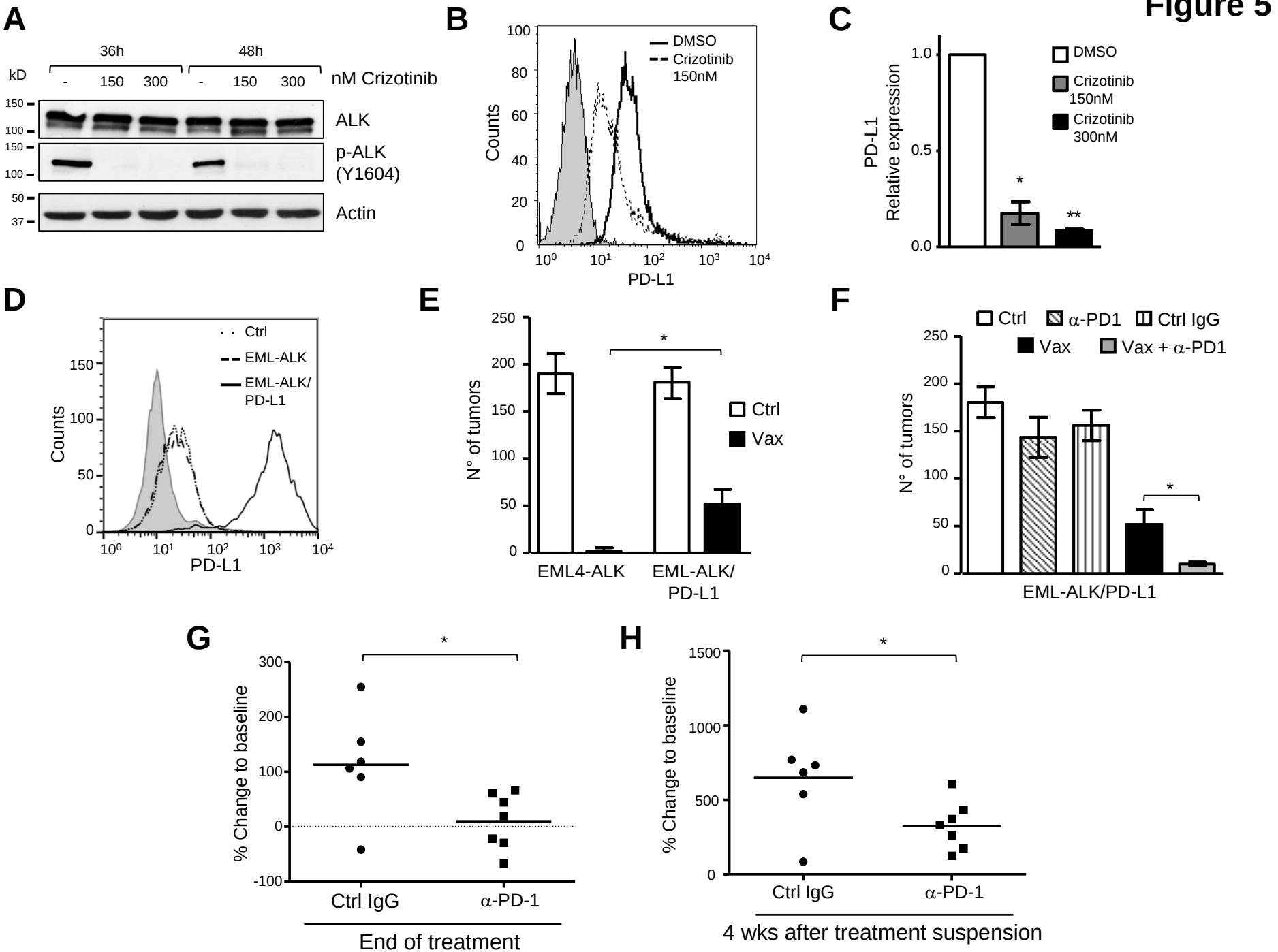
A
36h
48h
kD
- 150 300 - 150 300
nM Crizotinib
150
100
ALK
p-ALK (Y1604)
50
37
Actin
B
DMSO
Crizotinib 150nM
Counts
PD-L1
C
PD-L1 Relative expression
DMSO
Crizotinib 150nM
Crizotinib 300nM
*
**
D
Ctrl
EML-ALK
EML-ALK/ PD-L1
Counts
PD-L1
E
N° of tumors
*
Ctrl
Vax
EML4-ALK
EML-ALK/ PD-L1
F
Ctrl
α-PD1
Ctrl IgG
Vax
Vax + α-PD1
N° of tumors
*
EML-ALK/PD-L1
G
% Change to baseline
*
Ctrl IgG
α-PD-1
End of treatment
H
% Change to baseline
*
Ctrl IgG
α-PD-1
4 wks after treatment suspension

Figure 6

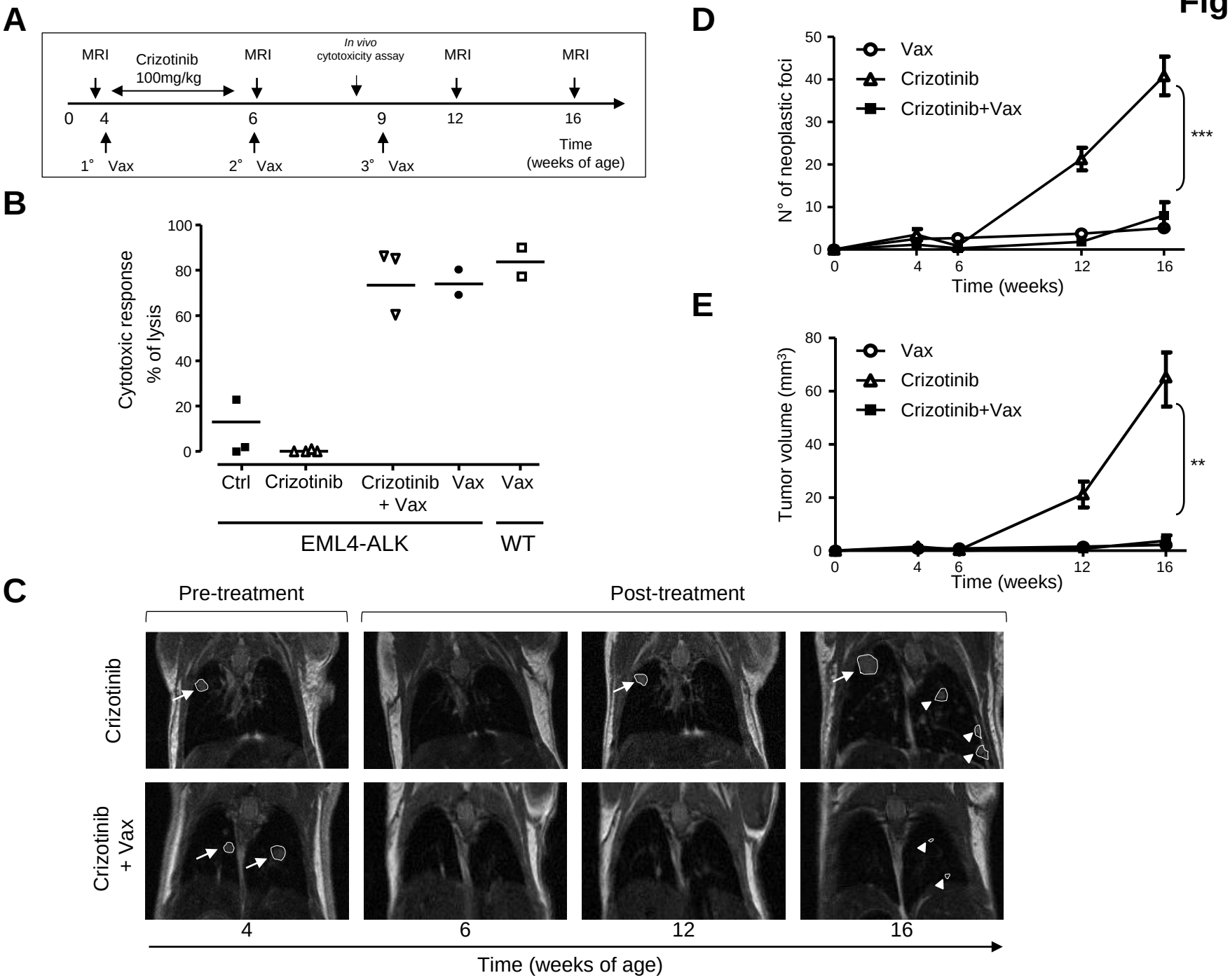
A
MRI
Crizotinib
100mg/kg
MRI
In vivo
cytotoxicity assay
MRI
MRI
0
4
6
9
12
16
Time
(weeks of age)
1° Vax
2° Vax
3° Vax
B
Cytotoxic response
% of lysis
100
80
60
40
20
0
Ctrl
Crizotinib
Crizotinib
+ Vax
Vax
Vax
EML4-ALK
WT
C
Pre-treatment
Post-treatment
Crizotinib
Crizotinib
+ Vax
4
6
12
16
Time (weeks of age)
D
N° of neoplastic foci
50
40
30
20
10
0
Vax
Crizotinib
Crizotinib+Vax
***
0
4
6
12
16
Time (weeks)
E
Tumor volume (mm3)
80
60
40
20
0
Vax
Crizotinib
Crizotinib+Vax
**
0
4
6
12
16
Time (weeks)

Figure 7

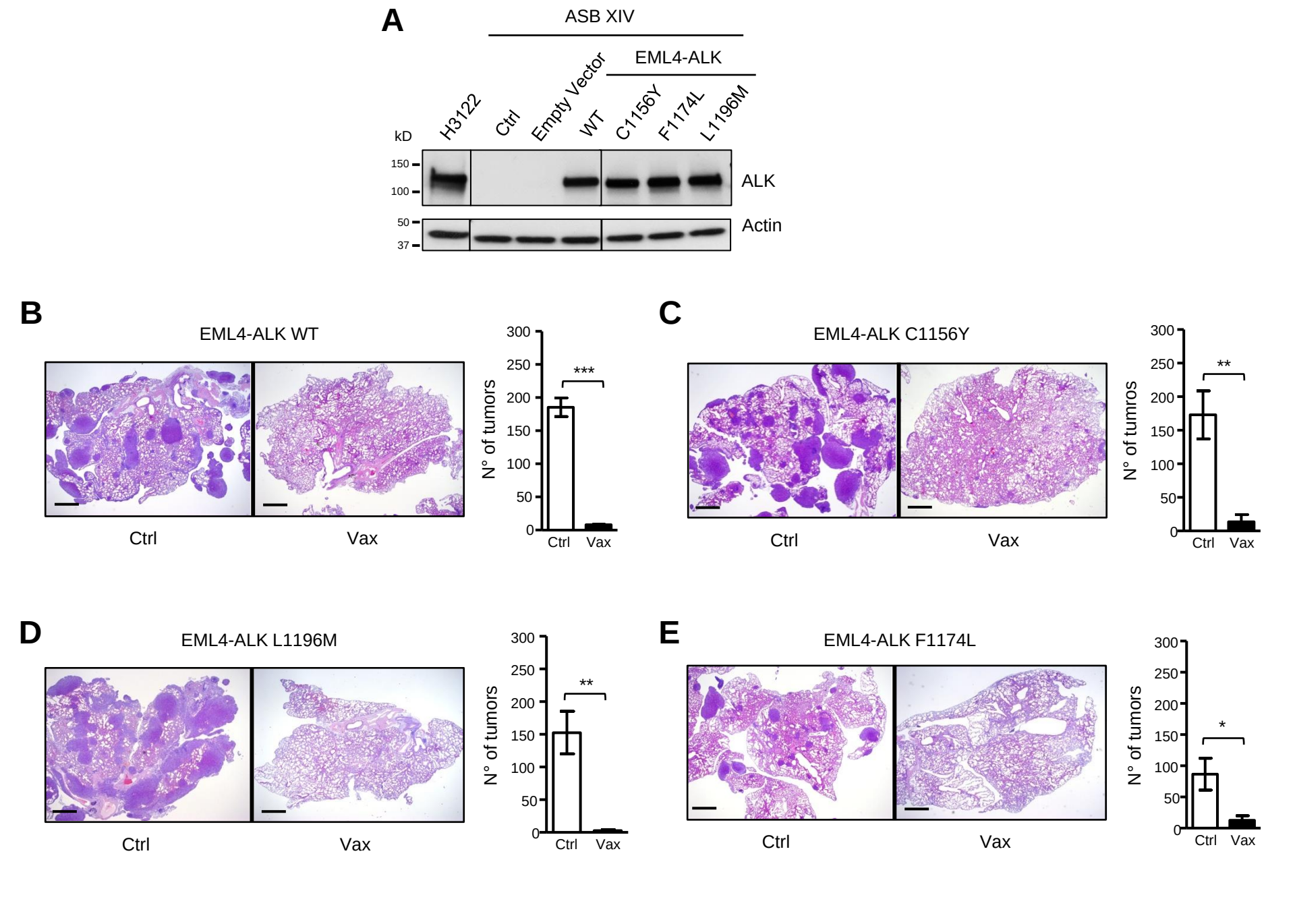
A
ASB XIV
EML4-ALK
H3122
Ctrl
Empty Vector
WT
C1156Y
F1174L
L1196M
kD
150
100
50
37
ALK
Actin
B
EML4-ALK WT
Ctrl
Vax
N° of tumors
300
250
200
150
100
50
0
***
C
EML4-ALK C1156Y
**
D
EML4-ALK L1196M
**
E
EML4-ALK F1174L
*